HHS Public Access

Author manuscript

Stem Cells. Author manuscript; available in PMC 2017 March 01.

Published in final edited form as:

Stem Cells. 2016 March ; 34(3): 732–742. doi:10.1002/stem.2232.

Arsenic Promotes NF-Kb-Mediated Fibroblast Dysfunction and Matrix Remodeling to Impair Muscle Stem Cell Function

Changqing Zhang[a], **Ricardo Ferrari**[a], **Kevin Beezhold**[b], **Kristen Stearns-Reider**[a], **Antonio D'Amore**[c], **Martin Haschak**[a], **Donna Stolz**[d], **Paul D. Robbins**[e], **Aaron Barchowsky**[b,f], and **Fabrisia Ambrosio**[a,g,h]

[a]Department of Physical Medicine and Rehabilitation, University of Pittsburgh, Pittsburgh, Pennsylvania, USA

[b]Department of Environmental and Occupational Health, University of Pittsburgh, Pittsburgh, Pennsylvania, USA

[c]Department of Bioengineering, University of Pittsburgh, Pittsburgh, Pennsylvania, USA

[d]Department of Cell Biology, University of Pittsburgh, Pittsburgh, Pennsylvania, USA

[e]Department of Metabolism and Aging, The Scripps Research Institute, Jupiter, Florida, USA

[f]Department of Pharmacology and Chemical Biology, University of Pittsburgh, Pittsburgh, Pennsylvania, USA

[g]McGowan Institute for Regenerative Medicine, University of Pittsburgh, Pittsburgh, Pennsylvania, USA

[h]Department of Physical Therapy, University of Pittsburgh, Pittsburgh, Pennsylvania, USA

Abstract

Arsenic is a global health hazard that impacts over 140 million individuals worldwide. Epidemiological studies reveal prominent muscle dysfunction and mobility declines following arsenic exposure; yet, mechanisms underlying such declines are unknown. The objective of this study was to test the novel hypothesis that arsenic drives a maladaptive fibroblast phenotype to promote pathogenic myomatrix remodeling and compromise the muscle stem (satellite) cell (MuSC) niche. Mice were exposed to environmentally relevant levels of arsenic in drinking water before receiving a local muscle injury. Arsenic-exposed muscles displayed pathogenic matrix remodeling, defective myofiber regeneration and impaired functional recovery, relative to controls. When naïve human MuSCs were seeded onto three-dimensional decellularized muscle constructs derived from arsenic-exposed muscles, cells displayed an increased fibrogenic conversion and

Correspondence: Fabrisia Ambrosio, Ph.D., M.P.T., Suite 308, Bridgeside Point Building II, 450 Technology Drive, Pittsburgh, Pennsylvania 15219, USA. Telephone: 412-624-5276; Fax: 412-624-9361; ambrosiof@upmc.edu.

Author contributions

C.Z., R.F., K.B., and A.D'A.: collection/assembly of data; data interpretation; manuscript writing; K.S.-R. and M.H.: collection/assembly of data; D.S. and P.R.: conception and design; data interpretation; A.B.: conception and design; data interpretation; manuscript writing; financial support; final approval of manuscript; F.A.: conception and design; collection/assembly of data; data interpretation; financial support; manuscript writing; final approval of manuscript.

Disclosure of Potential Conflicts of Interest

The authors indicate no potential conflicts of interest.

decreased myogenicity, compared with cells seeded onto control constructs. Consistent with myomatrix alterations, fibroblasts isolated from arsenic-exposed muscle displayed sustained expression of matrix remodeling genes, the majority of which were mediated by NF-κB. Inhibition of NF-κB during arsenic exposure preserved normal myofiber structure and functional recovery after injury, suggesting that NF-κB signaling serves as an important mechanism of action for the deleterious effects of arsenic on tissue healing. Taken together, the results from this study implicate myomatrix biophysical and/or biochemical characteristics as culprits in arsenic-induced MuSC dysfunction and impaired muscle regeneration. It is anticipated that these findings may aid in the development of strategies to prevent or revert the effects of arsenic on tissue healing and, more broadly, provide insight into the influence of the native myomatrix on stem cell behavior.

Keywords

Skeletal muscle; Muscle stem cells; Myofibroblast; Myogenesis; arsenic

Introduction

Chronic environmental exposure to arsenic (As(III)) in drinking water is a major public health hazard that affects the health of more than 140 million people worldwide. As(III) is odorless, colorless, and tasteless, rendering its effects pernicious. In addition to causing a number of cancers and non-cancer diseases (e.g., cardiovascular and pulmonary), chronic As(III) exposure causes significant muscle weakness and dysfunction [1–4]. Strikingly, sensorimotor impairment and muscle atrophy are observed in 10–14 million individuals exposed daily to As(III) in their drinking water [5, 6]. Despite the common finding of muscle weakness in As(III)-exposed individuals, the pathogenesis is poorly understood, as is how As(III)-exposure may affect an individual's ability to recover from an acute skeletal muscle injury. Although As(III) exposures affect large populations, the health impact of such environmental contaminants on adult tissue healing potential is not fully appreciated because, to date, the effect of metalloid exposure on stem cell function and tissue development has largely focused on embryonic or fetal models [7–11]. While mounting evidence demonstrates deleterious effects of metalloid exposure on stem cell function in developmental processes, the impact on critical roles that stem cells play in adult tissue growth and regeneration has thus far been neglected.

Muscle stem (satellite) cells (MuSCs) comprise a reserve cell population that normally resides in a quiescent state under conditions of skeletal muscle homeostasis. Following injury of young, healthy muscle, MuSCs are activated from a quiescent state and proceed through a sequence of proliferative expansion and myogenic differentiation to largely restore the original architecture and function of the damaged tissue [12, 13]. Although generally credited as the primary cells responsible for driving the regenerative cascade, MuSCs are reliant on biophysical and biochemical signals emanating from their immediate microenvironment, or niche, for appropriate activation [14, 15]. We and others have demonstrated that As(III) disrupts the myomatrix by promoting perivascular fibrosis in heart muscle [16–18] and driving ectopic lipid accumulation within the skeletal muscle [19]. While recent studies have focused on the direct effect of As(III) on MuSC metabolism and

behavior [4, 8–10], much less is known about the effect of As(III)-induced matrix alterations and pathogenic conversion of neighboring cell populations on tissue healing potential.

Muscle connective tissue (MCT) fibroblasts play a primary role in extracellular matrix (ECM) deposition and organization. Upon activation, these cells contain α-smooth muscle actin (αSMA) microfilaments, which form a stress fiber system within the cell that links to the ECM although a fibronexus and provides a mechanotransductive system for bi-directional communication between the cell and the matrix. This communication thereby drives a series of biochemical and biomechanical tissue responses. Activated fibroblasts, or myofibroblasts, serve to maintain tissue structural integrity and regulate myofiber regeneration [20, 21]. Studies by Kardon and colleagues recently demonstrated that ablation of the MCT fibroblast population drives a dysfunctional MuSC response to injury, as evidenced by a premature progression of MuSCs from proliferative expansion to terminal differentiation [20, 21]. Although the skeletal muscle microenvironment has been shown to become less supportive of cellular function with aging, immobility, and myopathy [22–24], it has not been extensively studied as a target for disease promotion from environmental exposures like As(III). In these studies, we demonstrate that As(III) exposure alters the muscle ECM to direct fibrogenic conversion of MuSCs. We also demonstrate that MCT fibroblasts isolated from As(III)-exposed muscle retain a phenotype with elevated expression matrix remodeling genes. The pathogenic fibroblast phenotype was concomitant with pathogenic matrix remodeling and an impaired regenerative response following an acute injury. However, pharmacologic inhibition of NF-κB, a transcription factor activated by cellular damage and stress, preserves normal muscle healing in As(III)-exposed animals, suggesting that NF-κB signaling may play an important role in the deleterious effect of As(III) on muscle regeneration.

Materials and Methods

Animal Exposure to As(III) in the Drinking Water

Six-week-old male wild type (C57Bl/6NTac) mice (Taconic Farms, Hudson, NY, USA) were exposed to 0 or 100 μg/l sodium metaarsenite ($NaAsO_2$) in their drinking water for 5 weeks. Arsenite was used as it is the most relevant toxic inorganic form of As(III). Fresh As(III)-containing water was provided every 2–3 days to insure that there is little As(III) oxidation to As(V). While human exposures to As(III) in drinking water ranges from negligible amounts to 1–4 mg/l, 100 μg/l is commonly accepted as a threshold for promoting a number of diseases and in dose ranging studies we found that this exposure was near maximal in promoting vascular tissue remodeling [25]. Our previous studies have demonstrated that these exposure levels do not cause any signs of overt lethality or changes in weight gain [4, 18, 19, 25]. All studies were approved by the Institutional Animal Care and Use Committee of the University of Pittsburgh. The mice are maintained on Prolab® Isopro® RMH3000.5P76 chow (LabDiet, St. Louis, MO) that is devoid of significant sources of inorganic arsenic.

Skeletal Muscle Injury

After 5 weeks of As(III) exposure, As(III) exposure was terminated and bilateral tibialis anterior (TA) muscles of the mice were injured with 10 μl of cardiotoxin (1.0 mg/ml). The right TA muscles from mice in each group were harvested and frozen in nitrogen-cooled 2-methylbutane (1 or 10 days post-injury) or preserved in scale view solution for second harmonics generation (SHG) imaging (10 days). For cell isolations, left TA muscles were used (3 days post-injury). An additional cohort of mice that received a muscle injury and were allowed to recover for 4 weeks (Fig. 5). After 4 weeks, in situ contractile testing was performed and muscles were subsequently harvested for (SHG) imaging.

In Situ Contractile Testing

In situ contractile testing of the anterior compartment muscles was performed in mice that were allowed to recover for 4 weeks after injury, as described previously [4, 26]. We chose the in situ method of functional testing because it allows for assessment of a single muscle compartment while maintaining normal orientation, innervation, and vascular supply. Muscle contractile properties, including peak twitch, peak tetanic force, time to peak twitch force, half relaxation time, fatigue resistance, and recovery from fatigue were quantified [27, 28].

Histology and Immunofluorescence

Frozen muscles were serially sectioned (12 μm) at −21 °C using a Thermo Scientific cryostat (Cryotome FSE Cyrostat, Thermo Scientific, Waltham, MA). Histological assessment of the recovery process was performed in groups of control and As(III)-exposed mice 1 day or 10 days after injury.

Evans Blue Dye—To assess the extent of injury and acute recovery 24 hours after cardiotoxin injections, Evans blue dye was administered by intraperitoneal (i.p.) injection. Slides were placed in cold acetone (−20 °C) for 1 minute and then air dried at room temperature (RT) (20 °C). The slides were immersed in xylene (22-050-283, Fisher Scientific, Waltham, MA) and mounted with DPx (44581 Sigma, Sigma-Aldrich, St. Louis, MO). Slides were imaged using an Olympus Fluoview 1000 confocal microscope (Olympus Fluoview FV1000, Olympus, Center Valley, PA) with the use of a Cy5 wavelength filter set to a wavelength of 625 nm. The number of Evans blue positive myofibers/field of view were identified by thresholding each image to a negative control (a site of no muscle injury) and automatically quantified using Elements AR (Nikon Elements AR, Nikon, Tokyo, Japan).

Laminin Immunofluorescence—Slides were washed three times with 1 × phosphate-buffered saline (PBS) and permeabilized with 0.03% Triton X-100 in PBS for 20 minutes at RT and subsequently blocked with 5% Normal Goat Serum (Vector S-1000, Vector Laboratories, Burlingame, Ca) diluted in PBS for 60 minutes. Slides were washed three times with 1 × PBS and three times with 0.5% bovine serum albumin (BSA), then incubated with Rat anti-Lamininα2 chainprimary (1:100, Abcam 11576, Cambridge, MA) for 60 minutes at RT. Slides were washed three times with 0.5% BSA and incubated with Goat anti-Rat Alexa Fluor 488 secondary (1:500, Life Technologies A-11006) for 60 minutes at RT. Slides were washed three times with 0.5% BSA, 3 × with 1 × PBS, and incubated with

4′,6-diamidino-2-phenylindole (DAPI) (Life Technologies 1370421, Thermo-Fisher) for 1 minute. Slides were washed six times with 1 × PBS and coverslips were mounted with Cytoseal XYL (Richard-Allen Scientific 8312-4, Thermo-Fisher). Slides were imaged using the Olympus Fluo-view 1000-1 confocal microscope. Myofiber diameter was determined using an automated macro written in Nikon Elements AR (Nikon Elements AR, Nikon, Tokyo, Japan).

SHG Imaging and Calculation of Collagen Fibril Orientation

To evaluate the effect of As(III) exposure on remodeling of the extracellular matrix following injury, we performed SHG imaging of injured muscles from control and As(III)-exposed animals. SHG imaging allows for 3D characterization of fibrillar collagen components of the ECM. Ten days or 4 weeks after injury, the TA was excised, placed in 2% paraformaldehyde for 2 hours, then in scale view solution for at least 1 week, and subsequently stored in PBS at 4 °C until imaged. All imaging was performed with an Olympus multi-photon microscope (Model FV1000, ASW software, Tokyo, Japan). The SHG signals were collected using back-scattered epidetectors. These detectors were non-descanned. Filters were provided by Chroma (chroma, Brattleboro VT). Before imaging, samples were placed in hanging drop slides in PBS and a coverslip was placed over the well, in contact with the muscle. The muscle was oriented with the superior border aligned parallel to the superior edge of the slide and the dorsal surface of the muscle against the coverslip. Images were taken of the medial and lateral muscle at the site of injury to a depth of 100 μm, with a step thickness of 2 μm and a scan pixel count of 1024_1024. Collagen fibers were visualized at an excitation bandwidth: 830 nm; myofibers were visualized at 500–550 nm.

A custom algorithm was used to quantify 3D fiber orientation of fibrillar collagen in SHG images of the site of active muscle fiber regeneration. The image analysis method has been described elsewhere and used on both native tissue [28] and artificial scaffolds [29]. Images from z-stack projections (500 μm × 500μm × 100 μm with a step of 2 μm) were analyzed using an algorithm based on an intensity gradient texture analysis, able to capture edges of the object of interest and identify their prevalent direction. A local thresholding segmentation method based on the collagen fibers characteristic length [28] was adopted to enhance the SHG signal against the noise. The orientation index (OI), as introduced previously [30], was used as a metric for the level of collagen fiber alignment. An OI equal to 0.5 corresponds to a network of isotropic fibers. In contrast, an OI equal to 1.0 indicates a perfectly aligned set of fibers. Volumetric analysis of myofibers from SHG images was calculated from 43 to 45 z-stack images/sample using NIS Elements software (Nikon Instruments). Three-dimensional (3D) reconstruction was performed using Imaris software (Version 8.1; Biplane, Concord, MA).

Skeletal Muscle Decellularization and Cell Seeding

Gastrocnemius muscles were harvested from animals 5 weeks after exposure to 0 or 100 μg/LAs(III) and decellularized using a modified procedure as described by Perniconi et al. [31]. Briefly, whole muscles were submerged in 1% SDS and placed on rotator at 200 rpm for 48 hours. SDS was replaced after 24 hours. Muscles were then washed in PBS for 1 hour,

autoclaved water for 1 hour, and followed by two washes in PBS for 30 minutes each. This decellularization process was confirmed by the absence of nuclear staining. Decellularized muscles were next transferred to culture media containing 88% Dulbecco's modified Eagle's medium (DMEM), 10% fetal bovine serum (FBS), 5% chick embryo extract (CEE; MP Biomedicals, Santa Ana, CA), and 1% penicillin/streptomycin (P/S).

Human MuSCs (hMuSCs; ScienCell Inc., Carlsbad, CA) were cultured in proliferation medium (DMEM containing 10% FBS, 10% horse serum, 0.5% CEE, and 1% P/S). We chose to use hMuSCs to demonstrate that the phenomenon being tested is human relevant. Flow cytometry analysis confirmed that these cells were >90% Pax7 positive, the canonical satellite cell marker ([32]; Supporting Information Fig. 1). On the day of cell seeding, whole decellularized gastrocnemius muscles were sectioned and placed into six-well plates. hMuSCs were trypsinized and resuspended in differentiation medium (DMEM containing 10% FBS, and 1% P/S) at concentration of 3×10^6 per milliliter, and seeded onto the muscle matrix. The six-well plates were then placed in cell incubator for 30 minutes to allow the cells to adhere. The wells were subsequently filled with 2ml differentiation medium. Media were changed every day for 4 days, after which time the hMuSC-ECM cultures were fixed in 2% PFA for 20 minutes, and transferred to 30% sucrose solution for 24 hours. The fixed tissues were then snap frozen in liquid nitrogen-cooled 2-methylbutane for 1 minute, and cryosectioned at 7 μm slices and mounted on glass slides. To characterize the phenotype of the differentiated hMuSCs seeded on the ECM, histological staining with desmin and transcription factor 4 (Tcf4) was performed. Sections were incubated overnight with either rabbit anti Tcf4 antibody (1:500, Cell Signaling, Danvers, MA) or rabbit anti-desmin antibody (1:1,000, Abcam, Cambridge, MA), followed by a 45-minute incubation with Alexafluor 488 goat anti-rabbit secondary antibodies (1:1,000, Life Technologies, Thermo-Fisher).

MCT Fibroblast Isolation and ECM Transcript Array

MCT fibroblasts were isolated from hind limb muscles of mice exposed to 0 or 100 μg/ LAs(III) for 5 weeks ($n = 8$ per group). Another cohort of mice exposed to 0 or 100 μg/ LAs(III) for 5 weeks were then subjected to a cardiotoxin muscle injury (as described above), and MCT fibroblasts were isolated from muscles 3 days post injury. In all groups, greater than 90% of the isolated cells stain positive for nuclear Tcf4 (data not shown), an indicator of interstitial MCT fibroblasts [20, 21]. After expansion of the cultures in the absence of As(III) for two passages, RNA was extracted from the four populations and assayed with an ECM-focused transcript array. Transcript abundance was normalized to a suite of house-keeping genes.

NF-κB Inhibition

To determine in vivo whether inhibition of NF-κB results in a reversal of the deleterious effect of As(III) on muscle regeneration, a cohort of mice were chronically treated with an eight lysine protein transduction domain (8K)/NEMO binding domain (8K-NBD) fusion peptide inhibitor of IKK (8K-NBD; 10mg/kg i.p. three times per week [33]) throughout the

See www.StemCells.com for supporting information available online.

time of exposure to 0 or 100 μg/l As(III). The eight lysine protein transduction domain/NEMO binding domain IKK/NF-κB, 8K-NBD (KKKKKKKKGGTALDWSWLQTE) was synthesized at the University of Pittsburgh Peptide facility. The peptide was dissolved in DMSO at 40 μM and stored at − 80°C until dilution in PBS directly before use. Control and As(III)-exposed mice were injected i.p. with vehicle (DMSO diluted in PBS) or 8K-NBD (10 mg/kg body weight) three times per week over 5 weeks. Injections were terminated at the time of cardiotoxin injury.

Statistical Analysis

All quantitative data are presented as means ± SD, unless otherwise indicated. Data were subjected to either one-tailed Student's *t*-test (when comparing Evans blue dye staining, Laminin α2 expression, collagen fiber orientation, and MuSC fate between control and As(III)-exposed groups), one-way analysis of variance (ANOVA) (when comparing specific tetanic force), or a two-way ANOVA (when comparing force frequency curves, fatigue resistance and recovery from a fatiguing protocol) to calculate the significance of group differences. Differences were considered statistically significant at $p \leq 0.05$.

Results

As(III) Exposure Impairs Muscle Regneration After an Acute Injury

One day after injury, there was no significant difference in the number of Evans blue dye positive fibers when comparing between the two experimental groups (Fig. 1A, 1C), suggesting that arsenic exposure does not render the muscle more susceptible to injury. However, after 10 days of recovery, there was a decrease in myofiber regeneration at the injury site of As(III)-exposed animals when compared with control counterparts(Fig. 1B, 1D). Quantitative analysis performed by digital image processing on muscles from As(III) animals displayed pathogenic matrix remodeling with injury, with increased collagen fibril alignment of As(III)-exposed animals, when compared with controls (Fig. 1E, 1G).

Consistent with histological evidence of an impaired regenerative response, a test of the contractile function of the anterior compartment using in situ contractile testing in live, anesthetized mice revealed that As(III) exposure results in a decreased specific tetanic force 4 weeks after injury (Fig. 2). The data indicate that As(III)-exposure compromises functional muscle repair following injury.

The Myomatrix of As(III)-Exposed Muscle Promotes a Fibrogenic Differentiation of MuSCs

Intrigued by the As(III)-induced alterations in the biophysical characteristics of the myomatrix and the corresponding impaired regeneration, we next investigated whether As(III)-induced ECM alterations may affect MuSC fate. hMuSCs seeded onto ECM isolated from As(III)-exposed muscle demonstrated decreased expression of desmin (a myogenic marker) and increased expression of Tcf4 (a transcription factor of fibroblasts) (Fig. 3), when compared with hMuSCs seeded onto control counterpart ECM constructs. These findings suggest that As(III)-induced alterations in the myomatrix promote fibrogenic differentiation of MuSCs and inhibit myogenicity.

MCT Fibroblast ECM Transcript Array

The gene expression of MCT fibroblasts isolated from animals exposed to 0 or 100μg/l As(III) for 5 weeks at 0 or 3 days post-injury was evaluated using an ECM transcript array. Of the 86 transcripts on the array, 25 transcripts for structural, protease, integrin, adhesion molecules, and regulatory proteins changed abundance with in vivo As(III) exposure. Twenty-one transcripts increased and four transcripts decreased by greater than a factor of two in MCT fibroblasts isolated from As(III)-exposed mice relative to expression in cells isolated from controls (Fig. 4).While many of the transcripts were changed in response to the injury alone, As(III) added to or synergized with the injury response to increase a predominance of NF-κB-transactivated genes (Fig. 4D relative to Fig. 4C). Notably, As(III) strongly increased expression of both matrix metalloproteinase 3 (Mmp3) and matrix metalloproteinase 13 (Mmp13). This expression was even greater in cells from injured, As(III)-exposed mice. These findings are consistent with an aberrant MCT fibroblast activation after injury that is characterized by a matrix-degrading phenotype, including the dramatic upregulation of thrombospondin-2 (Thbs2), a factor that drives NF-κB-mediated fibrosis [34, 35].The program of increased expression of proteases and structural proteins resembles that of the NF-κB-driven program that contributes to muscle decline in disease and aging [36–39].

Inhibition of NF-κB Improves Skeletal Muscle Regeneration in As(III)-Exposed Animals

Consistent with histological analysis 10 days after injury (Fig. 1), SHG imaging revealed that muscles from As(III)-exposed animals demonstrated an impaired myofiber regeneration that was characterized by disrupted myofiber integrity 4 weeks after injury (Fig. 5). While quantification of myofiber volume did not reveal significant differences across groups, there was significantly decreased peak specific tetanic force and impaired recovery from a fatiguing protocol of As(III)-exposed muscles, relative to controls (Fig. 6; Table 1).However, inhibition of NF-κB during As(III) exposure preserved the regenerative response as seen by full recovery of both muscle fiber morphology (Fig. 5), restored force-producing capacity and recovery from a fatiguing protocol (Fig. 6; Table 1). ECM arrays of transcripts from MCT fibroblasts isolated after 4 weeks of recovery from the As(III), 8K-NBD peptide, or As(III) plus 8K-NBD peptide exposed mice demonstrated that the levels of all of the transcripts shown in Figure 4 had returned to control levels in all of the groups (data not shown). This suggests that the altered ECM phenotype induced by arsenic and NF-κB during the exposure period was responsible for the poor recovery of function or tissue morphology, as opposed to a sustained alteration of matricellular gene expression. Taken together, these results suggest that environmentally common levels of As(III) exposure impairs functional healing of an acute muscle injury, and that targeting the NF-κB pathway may be beneficial in preventing muscle dysfunction accompanying chronic As(III) exposure.

Discussion

Skeletal muscle is characterized by an intricate extracellular matrix, which plays a critical role in the transmission of force. In the absence of sound matrix integrity, myofiber contractile capacity, and therefore, strength, is greatly diminished [40]. We [19, 25, 41] and others [16, 42] have observed profound dysfunctional tissue and matrix remodeling

following exposure to low level As(III) in multiple tissues. However, the pathogenesis for such modifications is unknown. This study provides mechanistic insight into these observations by demonstrating that As(III)induces MCT fibroblast dysfunction and a concomitant pathogenic myomatrix remodeling following an acute muscle injury. MCT fibroblasts isolated from As(III)-exposed muscle retain a phenotype with elevated expression of NF-κB-driven proteases and ECM proteins. Accordingly, As(III) signaling through NF-κB impairs post-injury force recovery following chronic As(III) exposure. Finally, we demonstrate that matrix alterations following exposure to As(III) exert direct effects on MuSCfate that may underlie the impaired tissue regenerative potential.

When naïve MuSCs were exposed ex vivo to 3D constructs derived from the myomatrix of animals exposed to As(III), we observed significantly decreased myogenicity of MuSCs and an increased Tcf4 + expression, suggesting a fibrogenic conversion. The advantage of the decellularization protocol used is that it maintains the topological complexity (architectural diversity) characteristic of the 3D native ECM as a substrate for cell seeding. Our findings that As(III)exposure impairs the regenerative response to an acute muscle injury are consistent with our previous investigations revealing that environmentally-relevant exposures of As(III) vitiates MuSC bioenergetics, as determined by high-resolution respirometry [4]. The altered oxygen consumption phenotype of As(III)-exposed cells was concomitant with aberrant mitochondrial morphology and an increased generation of reactive oxygen species [4]. Other studies have indicated direct arsenical actions on MuSCs that impair proliferation and myogenic differentiation [43, 44]. In vitro studies demonstrate that myoblasts exposed to As(III) in culture display a dose-dependent decrease in myotube formation and activation of the myogenic program [44]. Our novel findings suggest that biophysical and/or biochemical alterations of the physical microenvironment adversely affect MuSC regenerative potential in animals chronically exposed to As(III).

Stem cell behavior and function are largely determined by biophysical and biochemical cues emanating from the surrounding microenvironment [45]. Biophysical niche properties include matrix stiffness and architecture, for example, whereas biochemical cues involve cellular interactions and cytokine influences. Both biophysical and biochemical aspects of the niche have been shown to regulate stem cell activation, self-renewal, proliferation and differentiation [20, 46–48]. Findings from this study confirmed a pathogenic myomatrix architecture in animals exposed to As(III), and SHG with 3D reconstruction of injured muscles revealed that As(III) exposure resulted in a more aligned collagen fibril formation (Fig. 1E, 1G). Micro-structure-based models have shown that even small differences in the degree of fiber alignment may induce relevant mechanical anisotropy [49]. For example, considering a material with an elastic modulus of 7.5MPa, a 0.05 shift in the orientation index (OI) induces a 20%–30% strain difference between the two major material axes at a peak stress of 400 kPa [49]. Skeletal muscle from As(III)-exposed animals displayed a shift of nearly 0.09 in the OI, suggesting that exposure to As(III) dramatically alters skeletal muscle ECM biophysical properties.

The increased collagen fibril orientation observed in As(III)-exposed muscles is likely to contribute to the disorganized alignment of actively regenerating fibers, as observed in Figure 1E, 1G. At later time points after injury, the regenerating myofibers of animals

exposed to As(III) displayed a dramatically altered morphology which was characterized by a decreased myofiber density with a presumably compromised structural integrity (Fig. 5). These morphological alterations were consistent with a significantly decreased force producing capacity and fatigue resistance (Fig. 6).

Although previous studies have observed matrix remodeling in various tissues following As(III) exposure, the pathogenesis for such alterations remains largely unknown. MCT fibroblasts play a critical role in the production of matrix components, and recent findings have demonstrated that disrupted MCT fibroblast functioning at the site of an acute injury has been associated with impaired MuSC activation and decreased myofiber regeneration after injury [20, 21]. Fibroblasts are the primary cell type contributing to ECM synthesis following injury and, when unchecked, myofibroblast activity results in a pathogenic matrix deposition at the expense of functional myofiber regeneration [20, 21]. While MCT fibroblasts are generally activated in the presence of an acute lesion, it has been shown that the persistence of activated MCT fibroblasts, even in the absence of injury, may contribute to dramatic alterations in tissue structure and architecture [50]. In the liver, As(III) exposure was associated with an increased expression of αSMA-positive stellate cells, consistent with an upregulation of pre-fibrogenic cytokines, such as TGFβ, and collagen deposition [51]. Comparison of ECM-related gene expression in MCT fibroblasts isolated from control and As(III)-exposed mice revealed that As(III) induces a MCT fibroblast phenotype with sustained increased expression of collagen, elastin, and proteoglycan degrading proteases, matrix-devitalizing collagens, and pro-fibrotic regulatory factors. The majority of the increased transcripts share NF-κB transactivation (Fig. 4), and a consistent finding in cells isolated from As(III)-exposed uninjured or injured mice was four- to sixfold induction of Thrombospondin 2 gene (*Thbs2*) (Fig. 4), a known inducer of both NF-κB and fibrogenic repair [34, 35]. While it was not in the scope of the current studies to demonstrate that increased Thbs2 is essential for the As(III)-induced ECM remodeling, increased expression of Thbs2 is known to promote fibrosis and delay wound repair [34, 35, 52]. Thbs2 overexpression would also be consistent with the enhanced redox state of the muscle tissues that we have reported previously [4] and may also contribute to increased oxidants and oxidant-stimulated NF-κB in both the injured and uninjured state [34, 53].

NF-κB is an upstream inducer of, or a co-activator with, transcription factors important for fibrogenesis and metalloproteinase expression [37, 54, 55], and NF-κB activation by As(III) has been reported previously [56]. Here, we demonstrate in As(III)-exposed animals that pharmacological inhibition of NF-κB, through the use of the Nemo Binding Domain (NBD) peptide to inhibit IκB kinase (IKKγ), restores the regenerative response as determined by improved structural and functional muscle recovery that mimics that observed in non-exposed counterparts (Figs. (5 and 6)). IKK complexes promote degradation of IκB, thereby allowing for NF-κB translocation to the nucleus (reviewed in ref. [57]). Previous studies have demonstrated that blocking NF-κB or genetically eliminating NF-κB prevents muscle decline in a number of disease states, including cachexia and dystrophy, as well as in models of accelerated aging [36–39, 58]. In addition, dystrophic mice that were engineered to be heterozygously deficient for the p65 subunit of NF-κB displayed reduced inflammation and significantly increased myofiber regeneration when compared with controls.

Although our results indicate that As(III) exposure drives NF-κB activation in MCT fibroblasts, we cannot exclude the possibility that the enhanced functional recovery of As(III)-exposed muscles following inhibition of NF-κB is attributed to primary effects on other cell populations, including MuSCs. It was recently demonstrated that muscle progenitor cells isolated from RelA/p65$^{+/-}$ mice display enhanced cell proliferation and improved myogenic differentiation [59]. However, given the importance of appropriate MCT fibroblast functioning for MuSC responses and myofiber regeneration [20, 21], it is possible that enhanced the enhanced function observed in MuSCs isolated from RelA/p65$^{+/-}$ mice may be attributed, at least in part, to the fact that they resided in vivo in a more favorable biophysical environment, thereby enhancing intrinsic cell characteristics. The data in Figure 1E, 1G demonstrate that As(III) causes remodeling of the myomatrix (a property that is likely to be attributed to aberrant fibroblast function) before injury. Moreover, As(III) ECM remodeling before injury was sufficient to direct naïve MuSC towards fibrogenic differentiation. This would be consistent with recent findings by Cosgrove et al. demonstrating that substrate characteristics are important determinants of cell-intrinsic characteristics, including senescence, self-renewal and myogenicity [48]. Future studies should seek to further untangle the role of the myomatrix on MuSC behavior following chronic As(III) exposure as well as in other models of impaired muscle healing, including aging and myopathy. It is also probable that As(III)-induced MCT fibroblast alterations exert a direct effect on MuSC functioning, as multiple studies have shown the critical role of non-muscle cell populations in driving MuSC responses following an acute muscle injury [20, 60–62].

Summray

In summary, these studies demonstrate that environmentally relevant levels of As(III), found in the drinking water of millions of individuals worldwide, induces impaired skeletal muscle regeneration after injury and subsequent muscle weakness that is associated with upregulation of matrix remodeling genes in MCT fibroblasts. The implication is that a number of people who display a poor capacity for healing after injury, which may have previously been disregarded as insidious in nature, may be displaying adverse consequences of their environmental exposures. The findings suggest that NF-κB signaling serves as an important mechanism of action for the deleterious effects of As(III) on tissue healing, findings which may facilitate the future selection of strategies to prevent or revert the effects of As(III) on muscle maintenance and regenerative capacity. More broadly, we demonstrate that biophysical and biochemical characteristics of the native ECM influence stem cell fate, and may play an important role in dictating skeletal muscle regenerative capacity.

Acknowledgments

We thank Dr. Simon Watkins and Gregory Gibson at the Center for Biological Imaging for assistance with imaging. This work was supported by the NIH NIA Grant K01AG039477 (to F.A.), the Pennsylvania Department of Health/ Health Research Program (4100061184), the Pittsburgh Claude D. Pepper Older Americans Independence Center (P30AG024827), NIEHS Grant R01ES023696 (to F.A. and A.B.), NIEHS Grant R01ES013781 (to A.B.), NIEHS Grant F32ES022134 (to K.B.), and NIA grant P01AG43376 (to P.D.R.).

REFERENCES

1. Hughes MF, Beck BD, Chen Y, et al. Arsenic exposure and toxicology: A historical perspective. Toxicol Sci. 2011; 123:305–332. [PubMed: 21750349]
2. Moon KA, Guallar E, Umans JG, et al. Association between exposure to low to moderate arsenic levels and incident cardiovascular disease. A prospective cohort study. Ann Int Med. 2013; 159:649–659. [PubMed: 24061511]
3. Parvez F, Chen Y, Yunus M, et al. Arsenic exposure and impaired lung function. Findings from a large population-based prospective cohort study. Am J Respir Crit Care Med. 2013; 188:813–819. [PubMed: 23848239]
4. Ambrosio F, Brown E, Stolz D, et al. Arsenic induces sustained impairment of skeletal muscle and muscle progenitor cell ultra-structure and bioenergetics. Free Radic Biol Med. 2014; 74C:64–73. [PubMed: 24960579]
5. Chakraborti D, Mukherjee SC, Pati S, et al. Arsenic groundwater contamination in Middle Ganga Plain, Bihar, India: A future danger? Environ Health Perspect. 2003; 111:1194–1201. [PubMed: 12842773]
6. Mukherjee SC, Rahman MM, Chowdhury UK, et al. Neuropathy in arsenic toxicity from groundwater arsenic contamination in West Bengal, India. J Environ Sci Health A: Toxic/ Hazard Subst Environ Eng. 2003; 38:165–183.
7. Dakeishi M, Murata K, Grandjean P. Long-term consequences of arsenic poisoning during infancy due to contaminated milk powder. Environ Health. 2006; 5:31. [PubMed: 17076881]
8. Steffens AA, Hong GM, Bain LJ. Sodium arsenite delays the differentiation of C2C12 mouse myoblast cells and alters methylation patterns on the transcription factor myogenin. Toxicol Appl Pharmacol. 2011; 250:154–161. [PubMed: 20965206]
9. Hong GM, Bain LJ. Sodium arsenite represses the expression of myogenin in C2C12 mouse myoblast cells through histone modifications and altered expression of Ezh2, Glp, and Igf-1. Toxicol Appl Pharmacol. 2012; 260:250–259. [PubMed: 22426358]
10. D'Amico AR, Gibson AW, Bain LJ. Embryonic arsenic exposure reduces the number of muscle fibers in killifish (Fundulus heteroclitus). Aquat Toxicol. 2014; 146:196–204. [PubMed: 24316437]
11. Tokar EJ, Qu W, Waalkes MP. Arsenic, Stem cells and the developmental basis of adult cancer. Toxicol Sci. 2010; 120(suppl 1):S192–S203. [PubMed: 21071725]
12. Mauro A. Satellite cell of skeletal muscle fibers. J Biophys Biochem Cytol. 1961; 9:493–495. [PubMed: 13768451]
13. Brack AS, Conboy MJ, Roy S, et al. Increased Wnt signaling during aging alters muscle stem cell fate and increases fibrosis. Science. 2007; 317:807–810. [PubMed: 17690295]
14. Conboy IM, Conboy MJ, Wagers AJ, et al. Rejuvenation of aged progenitor cells by exposure to a young systemic environment. Nature. 2005; 433:760–764. [PubMed: 15716955]
15. Schultz E. Satellite cell behavior during skeletal muscle growth and regeneration. Med Sci Sports Exerc. 1989; 21:S181–S186. [PubMed: 2691829]
16. Hays AM, Lantz RC, Rodgers LS, et al. Arsenic-induced decreases in the vascular matrix. Toxicol Pathol. 2008; 36:805–817. [PubMed: 18812580]
17. Lantz RC, Chau B, Sarihan P, et al. In utero and postnatal exposure to arsenic alters pulmonary structure and function. Toxicol Appl Pharmacol. 2009; 235:105–113. [PubMed: 19095001]
18. Soucy NV, Mayka D, Klei LR, et al. Neovascularization and angiogenic gene expression following chronic arsenic exposure in mice. Cardiovasc Toxicol. 2005; 5:29–41. [PubMed: 15738583]
19. Garciafigueroa DY, Klei LR, Ambrosio F, et al. Arsenic-stimulated lipolysis and adipose remodeling is mediated by G-protein-coupled receptors. Toxicol Sci. 2013; 134:335–344. [PubMed: 23650128]
20. Murphy MM, Lawson JA, Mathew SJ, et al. Satellite cells, connective tissue fibroblasts and their interactions are crucial for muscle regeneration. Development. 2011; 138:3625–3637. [PubMed: 21828091]

21. Mathew SJ, Hansen JM, Merrell AJ, et al. Connective tissue fibroblasts and Tcf4 regulate myogenesis. Development. 2011; 138:371–384. [PubMed: 21177349]
22. Taylor-Jones JM, McGehee RE, Rando TA, et al. Activation of an adipogenic program in adult myoblasts with age. Mech Ageing Dev. 2002; 123:649–661. [PubMed: 11850028]
23. Kvist M, Hurme T, Kannus P, et al. Vascular density at the myotendinous junction of the rat gastrocnemius muscle after immobilization and remobilization. Am J Sports Med. 1995; 23:359–364. [PubMed: 7661268]
24. Christov C, Chretien F, Abou-Khalil R, et al. Muscle satellite cells and endothelial cells: Close neighbors and privileged partners. Mol Biol Cell. 2007; 18:1397–1409. [PubMed: 17287398]
25. Straub AC, Clark KA, Ross MA, et al. Arsenic-stimulated liver sinusoidal capillarization in mice requires NADPH oxidasegenerated superoxide. J Clin Invest. 2008; 118:3980–3989. [PubMed: 19033667]
26. Distefano G, Ferrari RJ, Weiss C, et al. Neuromuscular electrical stimulation as a method to maximize the beneficial effects of muscle stem cells transplanted into dystro-phic skeletal muscle. PloS One. 2013; 8:e54922. [PubMed: 23526927]
27. Cote CH, Ambrosio F, Perreault G. Metabolic and contractile influence of carbonic anhydrase III in skeletal muscle is age dependent. Am J Physiol. 1999; 276:R559–R565. [PubMed: 9950937]
28. Takanari K, Hong Y, Hashizume R, et al. Abdominal wall reconstruction by a regionally distinct biocomposite of extracellular matrix digest and a biodegradable elastomer. J Tissue Eng Regener Med. 2013
29. Sanchez-Palencia DM, D'Amore A, Gonzalez-Mancera A, et al. Effects of fabrication on the mechanics, microstructure and micromechanical environment of small intestinal submucosa scaffolds for vascular tissue engineering. J Biomechan. 2014; 47:2766–2773.
30. D'Amore A, Stella JA, Wagner WR, et al. Characterization of the complete fiber network topology of planar fibrous tissues and scaffolds. Biomaterials. 31:5345–5354. [PubMed: 20398930]
31. Perniconi B, Costa A, Aulino P, et al. The pro-myogenic environment provided by whole organ scale acellular scaffolds from skeletal muscle. Biomaterials. 2011; 32:7870–7882. [PubMed: 21802724]
32. Seale P, Sabourin LA, Girgis-Gabardo A, et al. Pax7 is required for the specification of myogenic satellite cells. Cell. 2000; 102:777–786. [PubMed: 11030621]
33. Tilstra JS, Robinson AR, Wang J, et al. NF-kappaB inhibition delays DNA damage-induced senescence and aging in mice. J Clin Invest. 122:2601–2612. [PubMed: 22706308]
34. Palenski TL, Gurel Z, Sorenson CM, et al. Cyp1B1 expression promotes angiogenesis by suppressing NF-kappaB activity. Am J Physiol Cell Physiol. 305:C1170–C1184. [PubMed: 24088896]
35. Calabro NE, Kristofik NJ, Kyriakides TR. Thrombospondin-2 and extracellular matrix assembly. Biochim Biophys Acta. 1840:2396–2402. [PubMed: 24440155]
36. Guttridge DC, Mayo MW, Madrid LV, et al. NF-kappaB-induced loss of MyoD messenger RNA: Possible role in muscle decay and cachexia. Science. 2000; 289:2363–2366. [PubMed: 11009425]
37. Wang H, Garzon R, Sun H, et al. NF-kappaB-YY1-miR-29 regulatory circuitry in skeletal myogenesis and rhabdomyosarcoma. Cancer Cell. 2008; 14:369–381. [PubMed: 18977326]
38. Reay DP, Yang M, Watchko JF, et al. Systemic delivery of NEMO binding domain/IKKc inhibitory peptide to young mdx mice improves dystrophic skeletal muscle histopathology. Neurobiol Dis. 2011; 43:598–608. [PubMed: 21624467]
39. Tilstra JS, Robinson AR, Wang J, et al. NF-kappaB inhibition delays DNA damage-induced senescence and aging in mice. J Clin Invest. 2012; 122:2601–2612. [PubMed: 22706308]
40. Wood LK, Kayupov E, Gumucio JP, et al. Intrinsic stiffness of extracellular matrix increases with age in skeletal muscles of mice. J Appl Physiol. 2014; 117:363–369. [PubMed: 24994884]
41. Soucy NV, Ihnat MA, Kamat CD, et al. Arsenic stimulates angiogenesis and tumori-genesis in vivo. Toxicol Sci. 2003; 76:271–279. [PubMed: 12970581]
42. States JC, Barchowsky A, Cartwright IL, et al. Arsenic toxicology: Translating between experimental models and human pathology. Environ Health Perspect. 2011; 119:1356–1363. [PubMed: 21684831]

43. Yen YP, Tsai KS, Chen YW, et al. Arsenic inhibits myogenic differentiation and muscle regeneration. Environ Health Perspect. 2010; 118:949–956. [PubMed: 20299303]
44. Steffens AA, Hong GM, Bain LJ. Sodium arsenite delays the differentiation of C2C12 mouse myoblast cells and alters methylation patterns on the transcription factor myogenin. Toxicol Appl Pharmacol. 250:154–161. [PubMed: 20965206]
45. Wang LD, Wagers AJ. Dynamic niches in the origination and differentiation of haematopoietic stem cells. Nat Rev Mol Cell Biol. 12:643–655. [PubMed: 21886187]
46. Engler AJ, Sen S, Sweeney HL, et al. Matrix elasticity directs stem cell lineage specification. Cell. 2006; 126:677–689. [PubMed: 16923388]
47. Gilbert PM, Havenstrite KL, Magnusson KE, et al. Substrate elasticity regulates skeletal muscle stem cell self-renewal in culture. Science. 2010; 329:1078–1081. [PubMed: 20647425]
48. Cosgrove BD, Gilbert PM, Porpiglia E, et al. Rejuvenation of the muscle stem cell population restores strength to injured aged muscles. Nat Med. 20:255–264. [PubMed: 24531378]
49. D'Amore A, Amoroso N, Gottardi R, et al. From single fiber to macro-level mechanics: A structural finite-element model for elastomeric fibrous biomaterials. J Mech Behav Biomed Mater. 39:146–161. [PubMed: 25128869]
50. Shi-Wen X, Chen Y, Denton CP, et al. Endothelin-1 promotes myofibroblast induction through the ETA receptor via a rac/phosphoinositide 3-kinase/Akt-dependent pathway and is essential for the enhanced contractile phenotype of fibrotic fibroblasts. Mol Biol Cell. 2004; 15:2707–2719. [PubMed: 15047866]
51. Ghatak S, Biswas A, Dhali GK, et al. Oxidative stress and hepatic stellate cell activation are key events in arsenic induced liver fibrosis in mice. Toxicol Appl Pharmacol. 2011; 251:59–69. [PubMed: 21134390]
52. Bancroft T, Bouaouina M, Roberts S, et al. Up-regulation of thrombospondin-2 in Akt1-null mice contributes to compromised tissue repair due to abnormalities in fibroblast function. J Biol Chem. 290:409–422. [PubMed: 25389299]
53. Tang Y, Scheef EA, Wang S, et al. CYP1B1 expression promotes the proangiogenic pheno-type of endothelium through decreased intra-cellular oxidative stress and thrombospondin-2 expression. Blood. 2009; 113:744–754. [PubMed: 19005183]
54. Lin X, Sime PJ, Xu H, et al. Yin yang 1 is a novel regulator of pulmonary fibrosis. Am J Respir Crit Care Med. 2011; 183:1689–1697. [PubMed: 21169469]
55. Charbonneau M, Harper K, Grondin F, et al. Hypoxia-inducible factor mediates hypoxic and tumor necrosis factor alpha-induced increases in tumor necrosis factor-alpha converting enzyme/ADAM17 expression by synovial cells. J Biol Chem. 2007; 282:33714–33724. [PubMed: 17884817]
56. Barchowsky A, Dudek EJ, Treadwell MD, et al. Arsenic induces oxidant stress and NF-kappa B activation in cultured aortic endothelial cells. Free Rad Biol Med. 1996; 21:783–790. [PubMed: 8902524]
57. Hayden MS, Ghosh S. Shared principles in NF-kappaB signaling. Cell. 2008; 132:344–362. [PubMed: 18267068]
58. He WA, Berardi E, Cardillo VM, et al. NF-kappaB-mediated Pax7 dysregulation in the muscle microenvironment promotes cancer cachexia. J Clin Invest. 123:4821–4835. [PubMed: 24084740]
59. Lu A, Proto JD, Guo L, et al. NF-kappaB negatively impacts the myogenic potential of muscle-derived stem cells. Mol Ther. 20:661–668. [PubMed: 22158056]
60. Cornelison DD. Context matters: In vivo and in vitro influences on muscle satellite cell activity. J Cell Biochem. 2008; 105:663–669. [PubMed: 18759329]
61. Mitchell KJ, Pannerec A, Cadot B, et al. Identification and characterization of a non-satellite cell muscle resident progenitor during postnatal development. Nat Cell Biol. 12:257–266. [PubMed: 20118923]
62. Uezumi A, Fukada S, Yamamoto N, et al. Mesenchymal progenitors distinct from satellite cells contribute to ectopic fat cell formation in skeletal muscle. Nat Cell Biol. 12:143–152. [PubMed: 20081842]

SIGNIFICANCE STATEMENT

Environmental toxicants, such as arsenic in drinking water, pose a significant and commonly encountered risk for causing skeletal muscle myopathies and atrophy; impairments that are among the greatest factors contributing to declines in functional mobility and strong predictors of mortality. Negative impact of chronic exposure to arsenic or other environmental toxicants on muscle stem cell biology and their local microenvironment represents an important pathogenic mechanism for reducing the capacity of these cells to maintain and regenerate muscle tissue. An improved understanding of arsenical effects on stem cell regenerative capacity in the etiology of arsenic-induced muscle weakness and fatigue will provide strategies for improving outcomes in patients in arsenic-endemic areas and for increasing basic knowledge of mechanisms through which environmental exposures impair stem cell function.

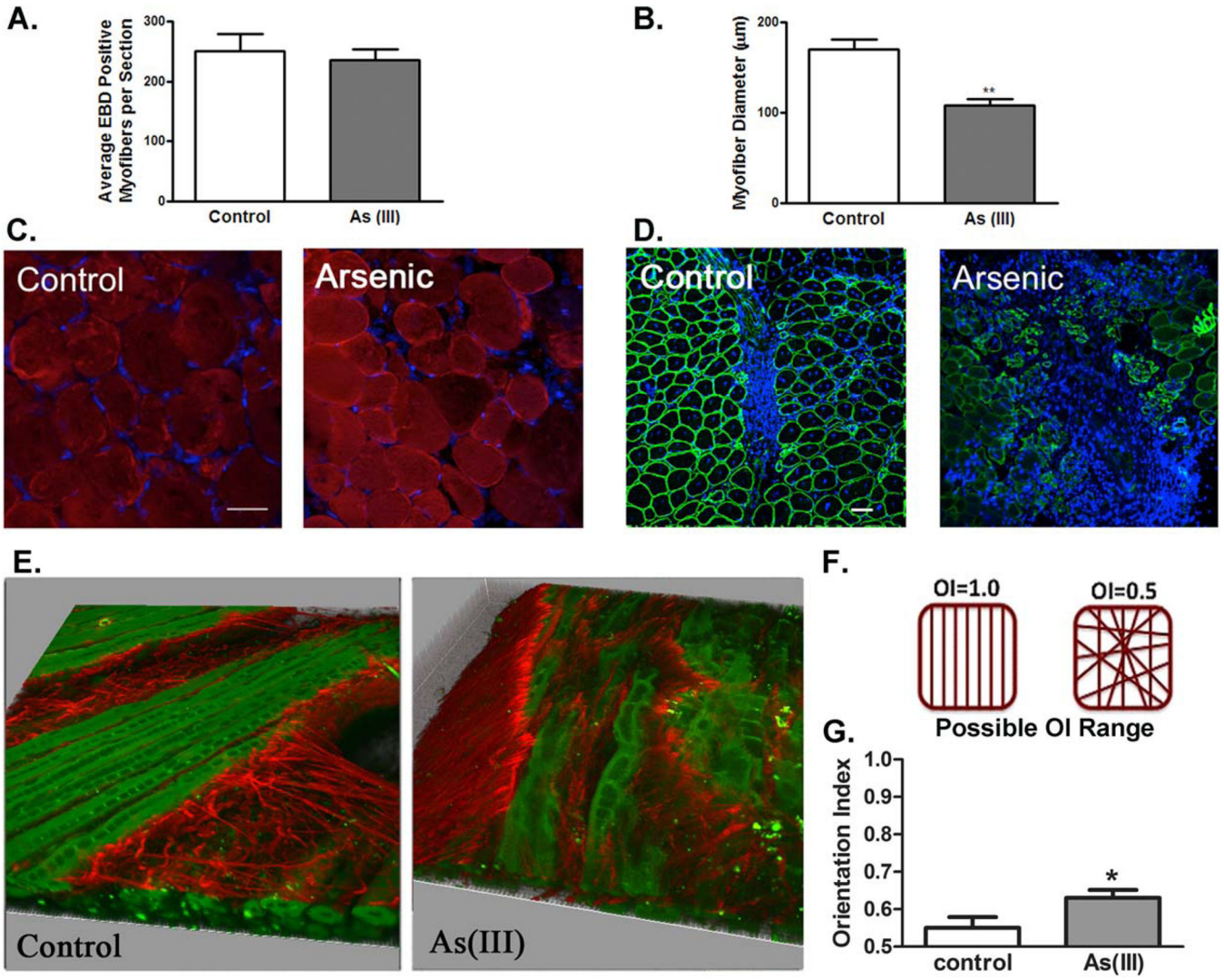

Figure 1.

Exposure to arsenic does not render the muscle more susceptible to injury, but results in a decreased regeneration and disrupted matrix deposition 10 days after injury. (**A**): The average number of Evans blue positive myofibers/cross-section in control and arsenic-exposed muscle after 1 day following cardiotoxin injection. (**B**): Average number of myofibers/cross-sectional area 10 days after cardiotoxin injection. (**C**): Evans blue auto-fluorescence in control and arsenic-exposed myofibers (red = Evans blue, blue = DAPI). n = 4 per group, $p > 0.05$ according to a two-tailed Student's t-test. Scale bar 5 100 μm. (D): Laminin α2 staining in control and arsenic-exposed muscles (green 5 Laminin α2, blue = DAPI). n = 4 per group, **, $p < 0.01$, according to a two-tailed Student's t-test. Scale bar 5 50 μm. (**E**):Second harmonics generation imaging of muscles exposed to 0 or 100 μg/ LAs(III) for 5 weeks reveals an impaired myo-fiber regeneration and disrupted matrix remodeling with exposure to As(III)(Collagen fibers in red; myofibers in green). Ten days after injury, As(III)-exposed muscles demonstrate an increased collagen fibril alignment, as calculated by the orientation index (OI). (**F**): Schematic representation of OI. (**G**): OI of

control and As (III) exposed muscles. ($n = 3$ in control and $n = 4$ in As (III) group, *, $p < 0.05$, 11– 13 stacked images/sample, right panel). Abbreviations: EBD, Evans blue dye; OI, orientation index.

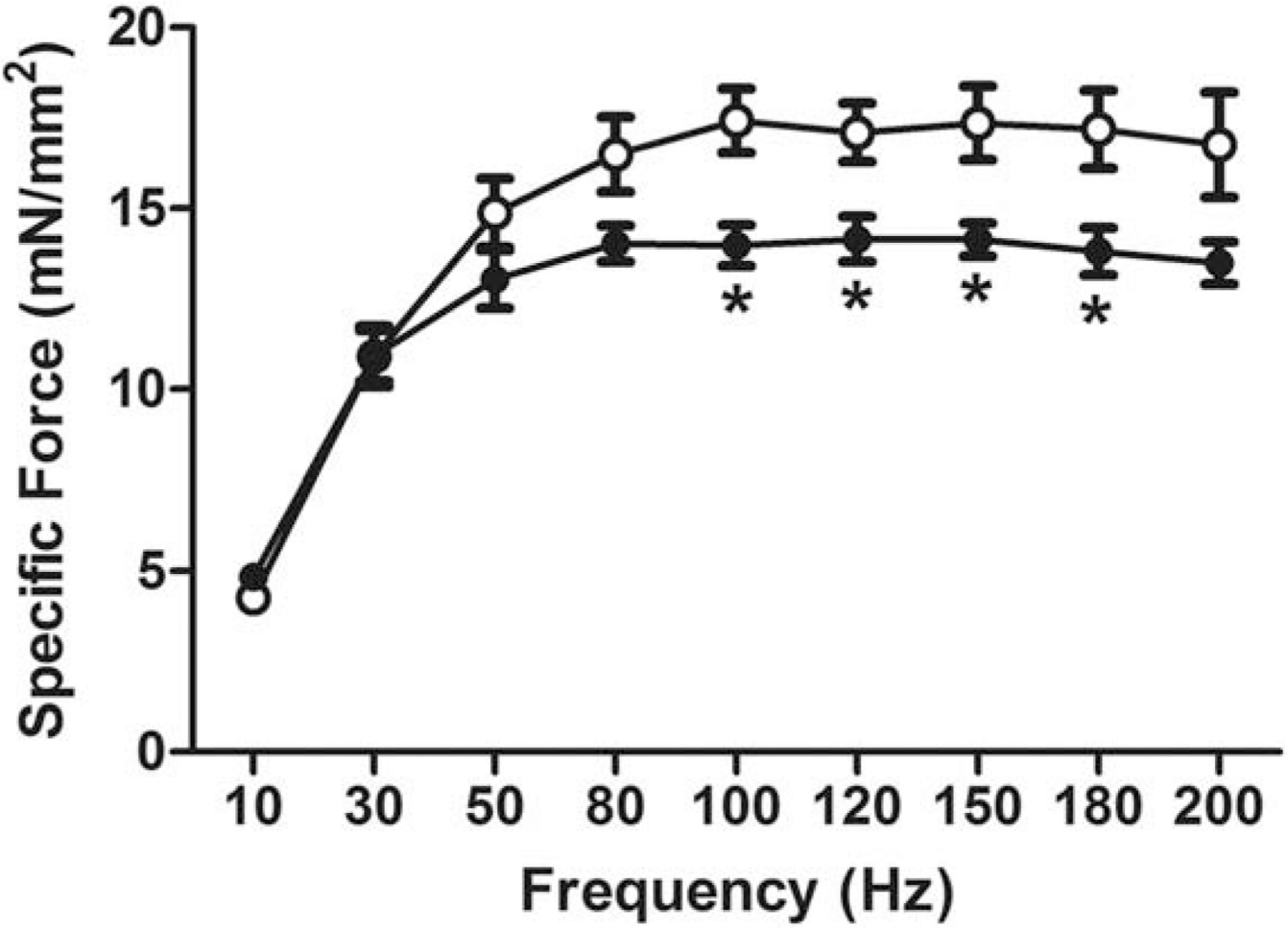

Figure 2.

As(III) exposure impairs recovery of muscle function four weeks after injury. Four weeks after cardiotoxin injury, in situ contractile testing of tetanic force production in the anterior leg muscle compartment was measured. Data are mean ± SEM of specific force for As(III)-exposed muscles (solid markers), compared with controls (open markers). *Significant difference when compared with control as determined by a one-way analysis of variance ($p < 0.05$, $n = 7–8$ per group).

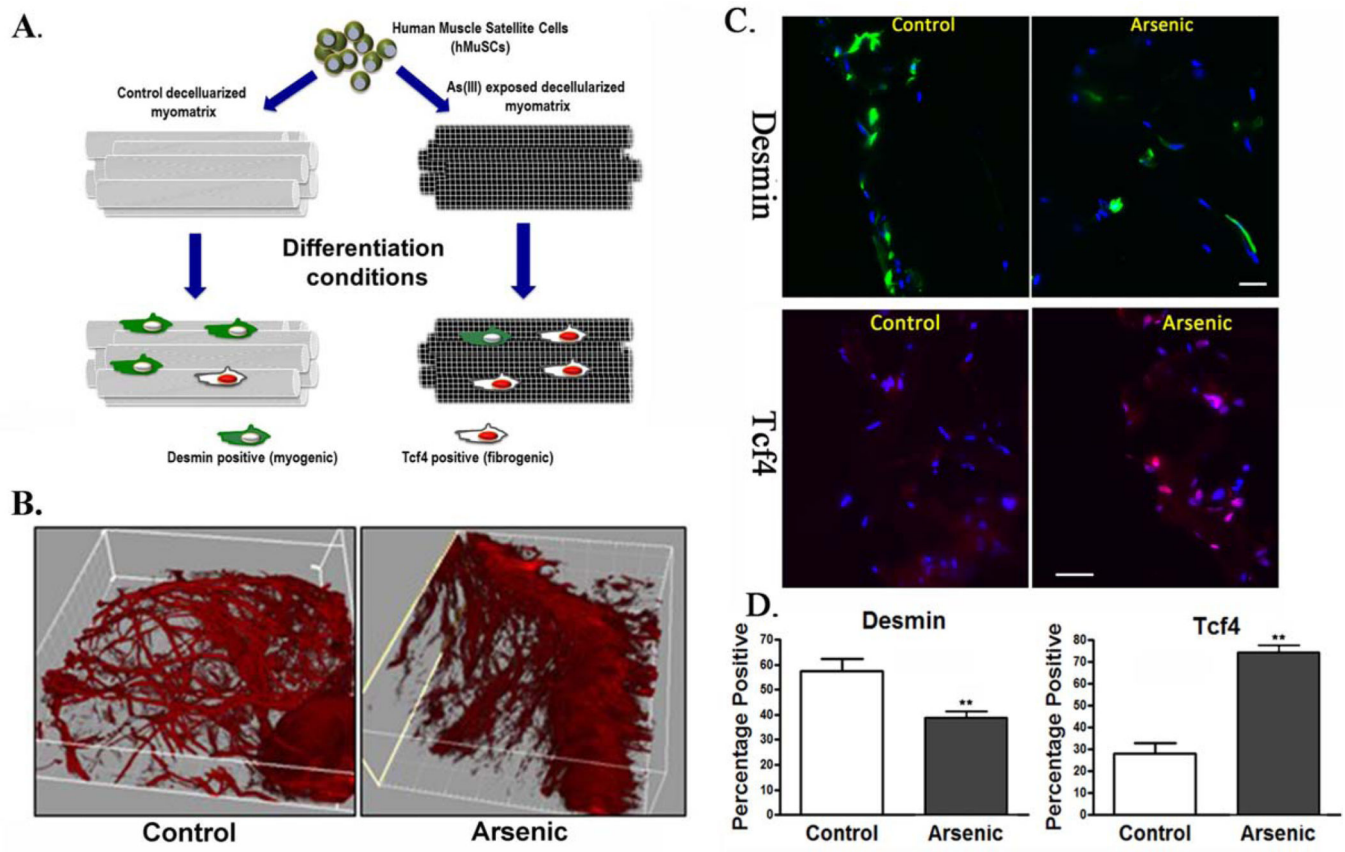

Figure 3.

The myomatrix from As(III)-exposed animals drives MuSC towards a fibrogenic lineage. Human MuSCs were seeded onto decellularized muscle constructs from animals exposed to 0 or 100 μg/LAs(III) for 5 weeks. Cell-seeded constructs were maintained in differentiation-promoting conditions for 3 days, after which time constructs were preserved for histological analysis of desmin or Tcf4 expression. (**A**): Schematic representation of experimental design. (**B**): Representative second harmonics generation images of decellularized muscle constructs derived from control and As(III)-derived constructs. (**C**): Immunofluroescence of desmin, a myogenic marker, (green), and Tcf4, a transcription factor of fibroblasts (red), of cells seeded onto decellularized matrices. (**D**): The percentage of cells staining positive for desmin or Tcf4 of cells seeded onto constructs derived from control or As(III)-exposed constructs, **, $p < 0.01$. Scale bars = 100 μm. Abbreviations: hMuSC, human muscle stem cell.

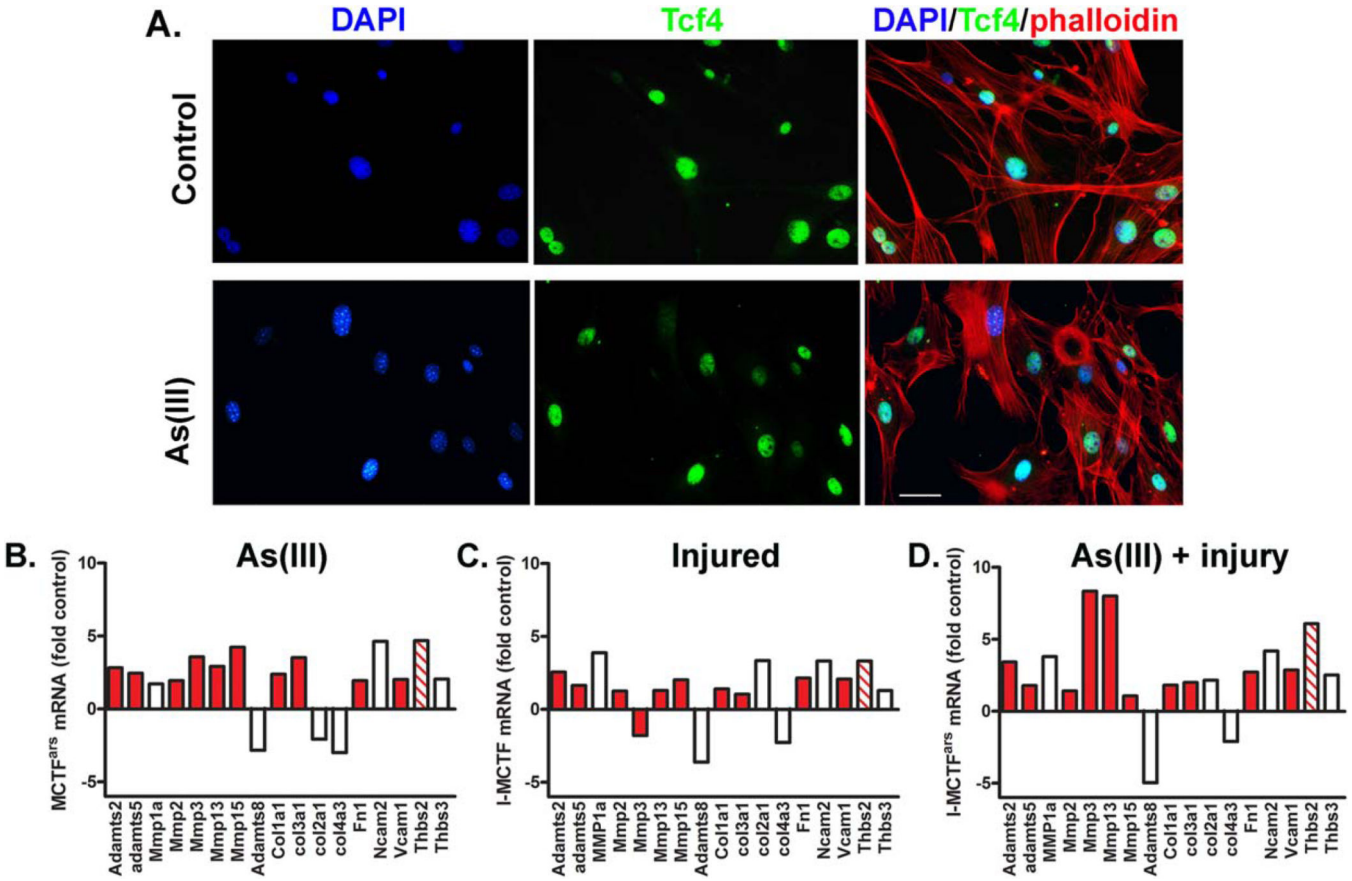

Figure 4.

Fibroblast extracellular matrix (ECM) transcript expression in recovery. MCT fibroblasts were isolated from control, injured, As(III)-exposed, or As(III)-exposed and injured mice. More than 90% of the cells were positive for Tcf4, a transcription factor of fibroblasts (**A**; Scale bar = 50 μm). (**B–D**): Cells were cultured for two passages in the absence of As(III) before RNA was isolated and transcripts were measured with an ECM-targeted quantitative polymerase chain reaction array. Transcript abundance was normalized to a suite of house-keeping genes and the graphs present the fold increase in transcripts in cells isolated from As(III)-exposed mice (**B**), injured mice (**C**), and As(III)-exposed, injured mice (**D**), relative to transcript abundance in uninjured, control mice. Red bars are NF-κB driven genes and the striped bar codes for Thbs2 that stimulates NF-κB. Abbreviations: DAPI, 4’,6-diamidino-2-phenylindole.

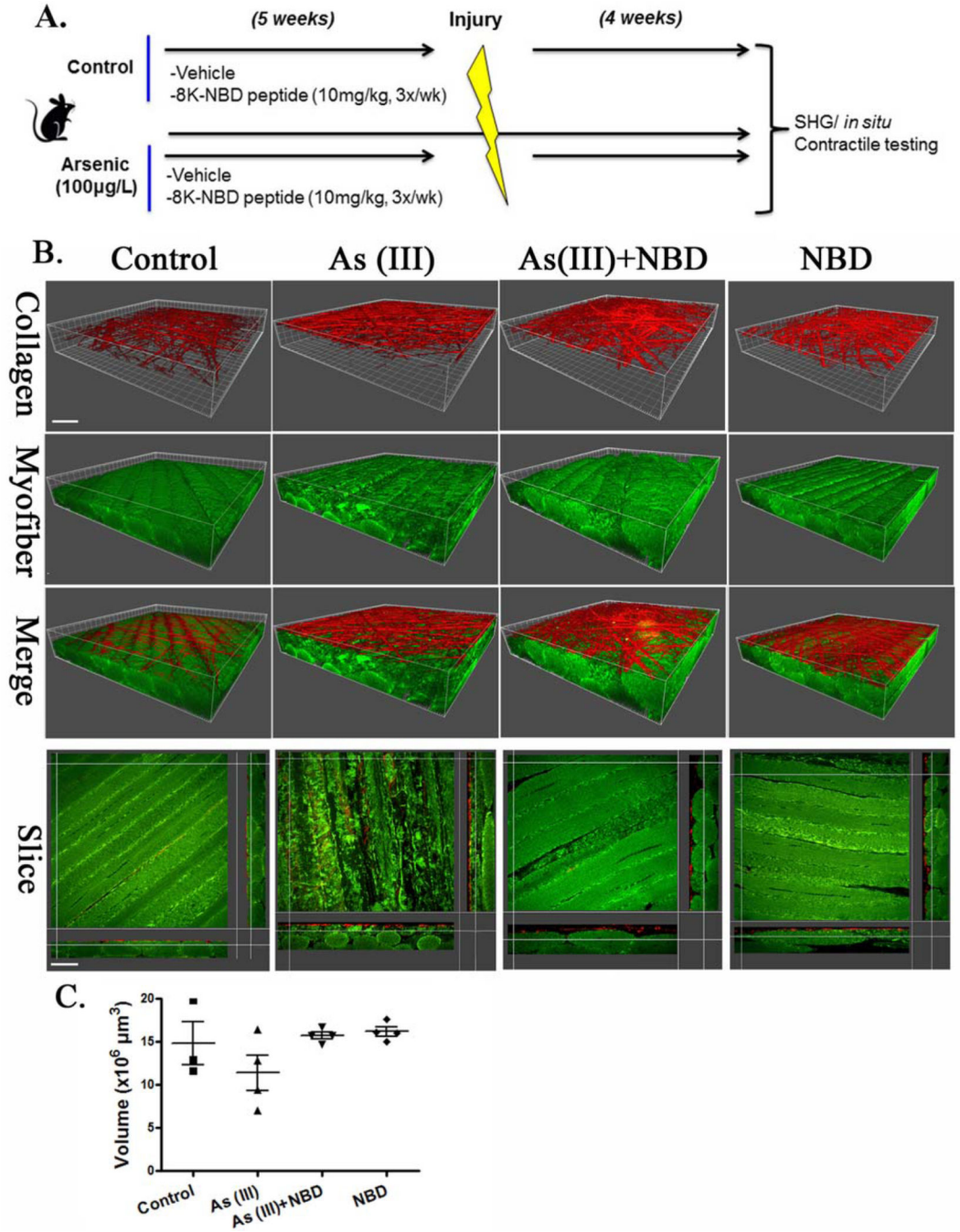

Figure 5.

As(III) exposure disrupts myofiber regeneration after injury. (**A**): Schematic representation of experimental design. A peptide inhibitor of NF-κB activation (eight lysine protein transduction domain (8K)/NEMO binding domain [8K-NBD]) was administered to control and As(III)-exposed mice for 5 weeks before cardiotoxin injury (vehicle = DMSO). After 4 weeks of recovery, functional testing of anterior muscle contractility and morphological analysis of muscle fibers were conducted. (**B**): Second harmonics generation imaging with 3D reconstruction of tibialis anterior muscle 4 weeks after injury. (**C**): Volumetric

quantification of myofibers across 4 experimental groups. Scale bar 5 upper left panel-40 μm, lower left panel-50 μm. Abbreviations: 8K-NBD, eight lysine protein transduction domain (8K)/NEMO binding domain; SHG, second harmonics generation.

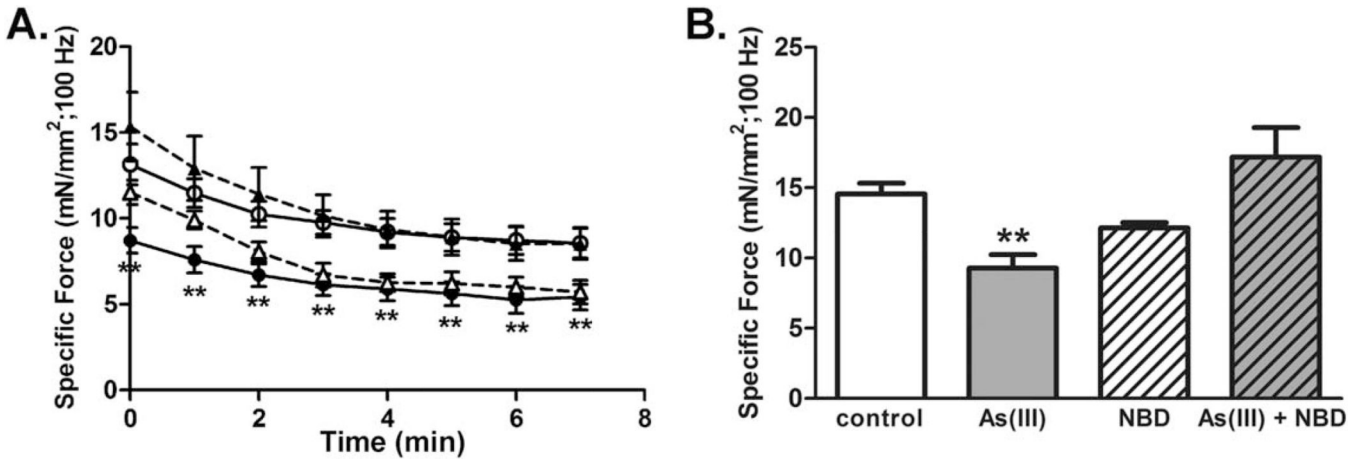

Figure 6.

Inhibition of NF-κB during As(III) exposure preserves skeletal muscle recovery after an acute injury. (**A**): In situ contractile testing 4 weeks after an acute injury revealed that As(III)-exposed muscles (closed circles, $n = 7$) displayed decreased specific tetanic force when stimulated at 100 Hz, relative to control (open circles, $n = 6$). The As(III)-exposed muscles also failed to recover to control levels of tetanic force by 10 minutes after fatigue (**B**). Inhibiting NF-κB with eight lysine protein transduction domain (8K)/NEMO binding domain (8K-NBD) peptide (open triangles, $n = 3$) during the exposure period did not affect the recovery from injury of specific force (**A**) or recovery from fatigue (**B**), relative to controls. However, inhibiting NF-κB in As(III)-exposed mice (closed triangles; $n = 4$), prevented As(III)-related decreases in all three muscle endpoints. **, $p < 0.01$. In (**A**), As(III) and 8K-NBD are significantly less than Control and As(III)+8K-NBD. In (**B**), As(III) is significantly different from control and As(III)+8K-NBD. Abbreviation: 8K-NBD, eight lysine protein transduction domain (8K)/NEMO binding domain.

Table 1

Arsenic and 8K-NBD inhibition on muscle and muscle contractile function

Measurement	Control	As(III)	As(III)+8K-NBD	8K-NBD	*p* value
Mice (*n*)	6	6	4	3	
Muscle weight (mg)	61.8 ± 2.4	54.5 ± 2.0	54.5 ± 5.5	52.3 ± 7.0	0.29
Muscle length (mm)	12.5 ± 0.1	11.9 ± 0.2[a]	12.5 ± 0.1	12.4 ± 0.1	0.04
Cross-sectional area (mm^2)	4.7 ± 0.2	4.3 ± 0.2	4.1 ± 0.4	4.0 ± 0.5	0.40
Maximum twitch torque (milliNm)	0.09 ± 0.01	0.09 ± 0.01	0.12 ± 0.01	0.12 ± 0.03	0.26
Maximum tetanic torque (milliNm)	1.43 ± 0.15	1.08 ± 0.12	1.45 ± 0.18	1.72 ± 0.18	0.08
Specific twitch force ($milliN/mm^2$)	4.04 ± 0.45	3.58 ± 0.22	4.03 ± 0.31	3.59 ± 1.29	0.85
Maximum specific tetanic force ($milliN/mm^2$)	10.2 ± 1.3	7.2 ± 1.0[b]	12.4 ± 0.2	15.1 ± 3.0	0.01
Frequency for maximum specific tetanic force (Hz)	75.0 ± 16.5	96.7 ± 18.6	90.0 ± 21.2	70.0 ± 10.0	0.73
Time to peak twitch (s)	0.35 ± 0.06	0.35 ± 0.05	0.27 ± 0.09	0.42 ± 0.06	0.53
Half-relaxation time (s)	0.170 ± 0.084	0.053 ± 0.029	0.002 ± 0.001	0.013 ± 0.007	0.17

Data are presented as the mean ± SEM and statistical differences were determined by standard one-way analysis of variance.

[a]Significantly different from Control;

[b]Significantly different from 8K-NBD.

Abbreviations: 8K-NBD eight lysine protein transduction domain (8K)/NEMO binding domain.